URSI GASS 2021, Rome, Italy, 28 August - 4 September 2021

Distance sensing using spiral resonators

Mahmoud Elgeziry*(1), and Filippo Costa(1), Simone Genovesi (1)
(1) Dipartimento Ingegneria dell'Informazione, Università di Pisa, Pisa, Italy

Abstract

A chipless RFID distance sensor is introduced. The sensor is based on a spiral resonator (SR) label printed on a dielectric substrate that is attached to the object to be sensed. The resonant structure is working at around 860 MHz, which is far from probing loop's self-resonant frequency. The change in the distance is tracked by observing the change in the sensor's behavior at resonance, in particular the change in the peak magnitude of the input impedance which is modulated by the distance between the spiral resonator tag and the probing loop. Preliminary data obtained from numerical simulations show that the proposed sensor is able to provide real-time remote sensing of the distance up to 20 mm with high resolution.

1 Introduction

There are different ways to measure the distance between two objects, each is characterized by a different set of hardware and degree of complexity. Depending on the application there might be the necessity of performing the distance measurement without any physical contact with the object to be sensed. Moreover, some issues are related to the reliability and the longevity of contact-based systems for example due to wear in case of mechanical contact, such as in a potentiometer. Non-contact based distance or proximity measurement has proved to be very useful in various applications such as parking sensors [1]–[3], health care [4], [5] and motion detection [6]. These solutions employ either Ultrasonic waves or Infrared-based sensing technologies to measure the distance between two objects.

Microwaves and millimeter waves (mm-waves) have found their way into several practical applications in wireless distance sensors, such as in the Inductive Proximity Sensors (IPS) technology which uses electromagnetic waves for wireless measurement of distance or position where the working principle is based on the fact that the proximity of a metal object changes in the impedance of the *sensing coil*, due to the generation of induction currents. The effect of the metal object in proximity may be quantified in terms of voltage, impedance, as well as frequency, these changes are then conditioned and processed by the evaluation electronics [7]. Some applications for IPSs are found in [7], [8] where the absence of a battery on the object to be measured was imposed as a constraint.

Radio Frequency Identification (RFID) technology has seen a drastic increase in the range of applications in the last few decades. Today, RFID is applied in fields such as: Automation, Retail, Agriculture, and various other industrial applications. This boom in the technology has attracted researchers and engineers to develop new and innovative applications using RFID, as summarized in the following review paper [9].

Some RFID systems offer more than just identification such as the so-called sensor-enabled tags which are capable of not only identifying objects but also reacting to the change in a physical property in their working environment. Applications, including commercially available, involving RFID sensor-enabled tags for Humidity, Temperature, Pressure, or Weight measurements can be found in [10]. A quick examination of the literature shows the emerging technology of using chipless of RFID-based systems by using tags that are completely passive in a wide range of applications such as [11], [12]. The absence of a microchip, which is the main component in traditional RFID tags, in chipless tags has several advantages, including a significant reduction in the cost of the tag and the possibility to be suitable even for harsh working environments where IC (integrated circuit)-based RFID tags suffer. Chipless RFID tags are often made of resonant elements such as Split Ring Resonators [13] or Spiral Resonators [14], sometimes referred to as metamaterial surfaces. The working principle behind a chipless RFID sensor measurement can be based on the response at resonance due to a change in the physical parameter to be measured. These metamaterial-based chipless RFID sensors track the changes in the resonant frequency or the magnitude of the resonance peak to determine the change in the measurand.

In this paper we present a wireless distance sensor based on a probing loop as reader, fed with a fixed frequency, coupled with a chipless RFID tag realized with spiral resonant inclusion where the distance is obtained by measuring the change in the impedance of the probe loop which will be modulated by the change in the distance between the reader and the tag. The proposed sensor offers several advantages over the previously cited works such as: simple circuitry, inexpensive, and small size footprint. The range of distance that can be measured depends on the maximum allowable distance for coupling between the reader and the tag, however the design can be scaled easily to be suitable for applications requiring larger ranges. The system herein described can be used to extract information

about the relative distance between the reader and the tag. This device can have applications in various fields, for example as an industrial application this system can be used as a contactless limiting switch. Another potential application is in Structural Health Monitoring (SHM) providing a continuous real time report on the status of a structure. Finally, it can also be integrated as a wearable device for health care sensors.

2 Design

The objective is to measure the distance between the tag and a fixed point (the probe loop reader) using passive chipless tags. The proposed tag is based on a Spiral Resonator (SR) magnetic inclusion presented in [15]. Circular and Rectangular/Square SRs are the most conventional geometries found in the literature, in this work a square SR, shown in figure 1, is adopted because it is more suitable for sensing applications [16] .

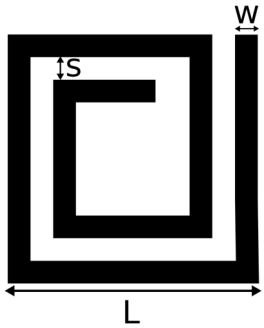

Figure 1. 2-turn Spiral Resonator magnetic inclusion with trace width (*w*), trace separation (*s*), and side length (*L*).

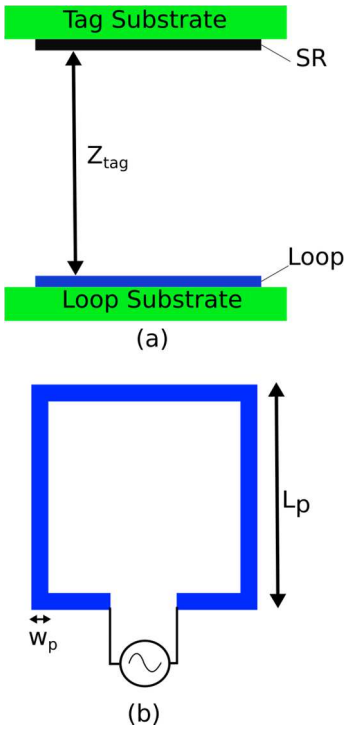

Figure 2. (a) Schematic layout of the proposed sensor **(b)** top view of the square probing loop having a side length (L_p).

The two-turn square SR with side length *L*, trace width *w*, and trace separation *s*, is realized on a dielectric substrate and embedded in the full set-up of the sensor shown in figure 2 which includes in addition a square probing loop whose side length is denoted by L_p, and metallization thickness w_p, realized on an identical dielectric substrate. The idea is that the input impedance of the probing loop is a function of the vertical displacement of the SR-carrying tag (Z_{tag}). This is because the coupling between the tag and the reader is depends on the distance between them.

The system is based on the principle of electromagnetic induction where the loop produces a magnetic field varying in polarity according to the feeding frequency of the loop. If the spiral resonator is in proximity of the loop, this varying magnetic field generates a current in the SR that tries to oppose the original field. The working frequency is determined according to the self-resonant frequency of the SR which is dependent on its geometry, dimensions, and the mutual coupling with the loop. At the resonant frequency, the SR behaves as a lumped RLC resonant circuit, as shown in figure 3, where the probing loop is modelled as an inductance in series with a resistance, while the SR is modelled as a series RLC circuit. The lumped parameters consideration is valid since the electrical size of the SR at resonance is small. The evaluation of the lumped parameters Resistance R_{SR}, Self-Inductance L_{SR}, Capacitance C_{SR}, and Mutual Inductance *M* is out of the scope of this paper and is discussed extensively in the literature. [17]–[20].

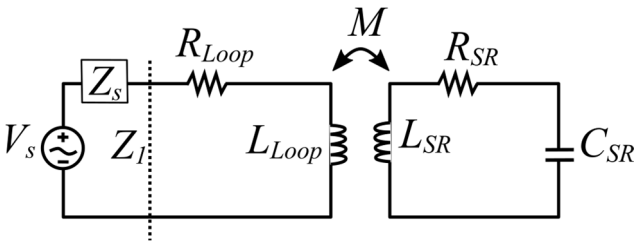

Figure 3. Equivalent circuit model for the proposed sensor showing the probing loop (left side) and the SR (right side) coupled together by the mutual inductance term M.

An expression for the input impedance (Z_I) of the overall circuit is expressed in terms of the lumped parameters shown in figure 3 according to [17] as

$$Z_1 = R_{Loop} + j\omega L_{Loop} + \frac{\omega^2 M^2}{j\omega L_{SR} + \frac{1}{j\omega C_{SR}} + R_{SR}}. \quad (1)$$

The impedance (Z_I) has a local maximum at the operating frequency due to the resonant behaviour introduced by the SR whose value depends strongly on the mutual inductance *M* between the tag and the loop which is a function in the distance between them. Therefore, this can be exploited to obtain a distance measurement by looking at the input impedance at resonance. Of course, if this distance exceeds

a certain value, this coupling becomes null and the measured impedance is only due to the probing loop (*i.e.* no longer varies as the tag goes farther away from the reader).

3 Numerical Results

The proposed sensing concept of the system shown in figure 2a was verified using full wave simulations on Computer Simulation Technologies (CST) Microwave Studio [21]. The two-turn spiral resonator with side length ($L = 18\ mm$), metallization width (w = 1.5 mm), separation ($s = 2\ mm$) was etched on a square 50x40 mm 1.6 mm-thick FR-4 substrate. The tag was interrogated by a square probing loop of side length (L_p = 22 mm) and metallization width (w_p = 2 mm), accommodated on a substrate of the same size as the one of the SR tag. The value of the input impedance was observed as the tag-reader distance was varied from 10 mm to 20 mm.

Figure 4 below shows the real part of the input impedance at the input terminals of the loop versus frequency as the distance between the tag and the loop (Z_{tag}) varies. Z_l clearly exhibits resonance at around 866 MHz due to the introduction of the resonant behaviour of the SR placed in close proximity. The plot shows the decrease of the maximum value of the real impedance as the distance to the tag increases owing to the decrease in the tag-reader mutual inductance.

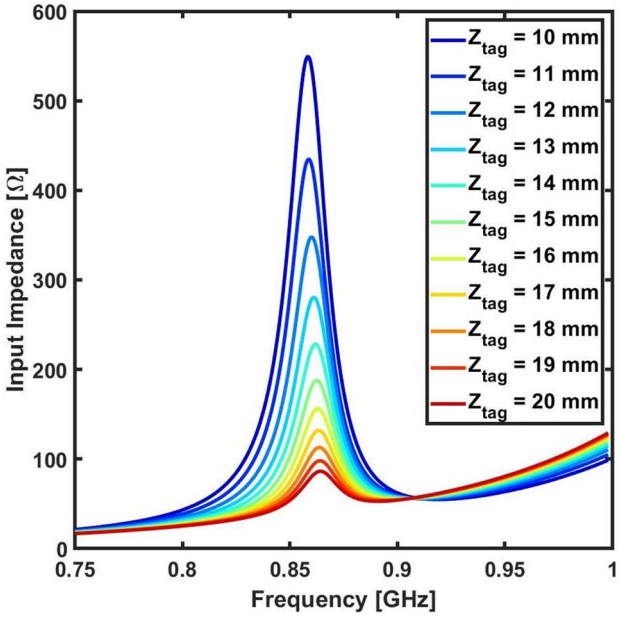

Figure 4. Real Input impedance versus frequency at various values of Z_{tag} for L_p = 22 mm, w_p = 2 mm, L = 18 mm, w = 1.5 mm, s = 2 mm, and N = 2 turns

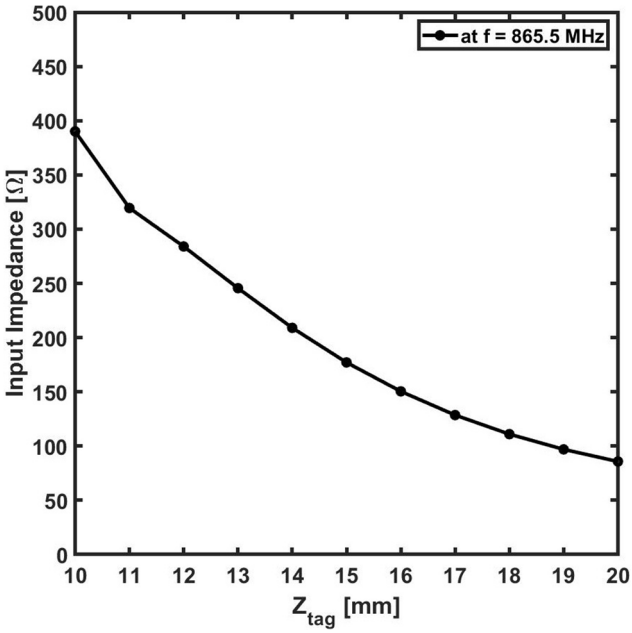

Figure 5. Real Input impedance at 865.5 MHz for a varying tag-reader distance (Z_{tag}) for the same dimensions reported in figure 4.

To present the results in a more meaningful way, and also to demonstrate the potential for scalability, figure 5 shows the variation of the real input impedance of the loop versus the distance to the tag at a fixed frequency of 865.5 MHz. It can be seen from the plot that the real input impedance $\mathrm{Re}\{Z_l\}$ of the probing loop decreases as the tag moves away from the reader until it approaches saturation at around 20 mm. The maximum readable distance can be increased if the size of the SR is increased. The proposed method allows extracting a relationship between the change in the tag-reader distance and the input impedance measured by the reader.

4 Conclusion

This paper presents a simple and inexpensive chipless Radio Frequency (RF) system capable of sensing changes in the distance between two objects. The system is based on a spiral resonator and a probing loop as reader, both realized on an FR-4 substrate. The decrease in the mutual inductance between the tag and the reader is exploited to obtain a distance measurement. This setup can sense distances up to 20 mm with a high resolution. This device is characterized by its durability since there is no physical contact between the tag and the reader. Moreover, the results obtained show that it is possible to adapt the device to applications requiring a different operating frequency or a sensing range. The presented solution offers an advantage over its counterparts, relying on other technologies, because of its consistent functionality in various conditions such as dusty environments or presence of other obstacles between the tag and the reader that might interfere with the measurement from a sensor based on another technology. Another key advantage is the possibility of interrogating the reader at a single-frequency and obtain a relationship

between the measured real part of the input impedance and the distance between the tag and the reader.

5 References

1. O. Sajdl, J. Zak, and R. Vrba, 'Zigbee-Based Wireless Distance Measuring Sensor System', in Personal Wireless Communications, Boston, MA, 2007, pp. 403–409, doi: 10.1007/978-0-387-74159-8_40.

2. J. P. Benson et al., 'Car-Park Management using Wireless Sensor Networks', in Proceedings. 2006 31st IEEE Conference on Local Computer Networks, Nov. 2006, pp. 588–595, doi: 10.1109/LCN.2006.322020.

3. A. von Reyher, M. Naya, and H. Chiba, 'Parking assist system', US8319663B2, Nov. 27, 2012.

4. A. Ghosh et al., 'On automatizing recognition of multiple human activities using ultrasonic sensor grid', in 2017 9th International Conference on Communication Systems and Networks (COMSNETS), Jan. 2017, pp. 488–491, doi: 10.1109/COMSNETS.2017.7945440.

5. T. Hori and Y. Nishida, Ultrasonic Sensors for the Elderly and Caregivers in a Nursing Home. .

6. J. Yun and M. Song, 'Detecting Direction of Movement Using Pyroelectric Infrared Sensors', IEEE Sens. J., vol. 14, no. 5, pp. 1482–1489, May 2014, doi: 10.1109/JSEN.2013.2296601.

7. B. George, H. Zangl, T. Bretterklieber, and G. Brasseur, 'A Combined Inductive–Capacitive Proximity Sensor for Seat Occupancy Detection', IEEE Trans. Instrum. Meas., vol. 59, no. 5, pp. 1463–1470, May 2010, doi: 10.1109/TIM.2010.2040910.

8. P. Kejík, C. Kluser, R. Bischofberger, and R. S. Popovic, 'A low-cost inductive proximity sensor for industrial applications', Sens. Actuators Phys., vol. 110, no. 1, pp. 93–97, Feb. 2004, doi: 10.1016/j.sna.2003.07.007.

9. A. N. Nambiar, 'RFID Technology: A Review of its Applications', 2009.

10. F. Bertuccelli, A. Colonna, W. Malik, D. Ranasinghe, and T. López, 'Sensor-enabled RFID tag handbook', Jan. 2008.

11. M. Borgese, F. A. Dicandia, F. Costa, S. Genovesi, and G. Manara, 'An Inkjet Printed Chipless RFID Sensor for Wireless Humidity Monitoring', IEEE Sens. J., vol. 17, no. 15, pp. 4699–4707, Aug. 2017, doi: 10.1109/JSEN.2017.2712190.

12. F. Costa et al., 'Wireless Detection of Water Level by Using Spiral Resonators Operating in Sub-Ghz Range', in 2019 IEEE International Conference on RFID Technology and Applications (RFID-TA), Sep. 2019, pp. 197–200, doi: 10.1109/RFID-TA.2019.8892141.

13. J. Naqui and F. Martín, 'Application of broadside-coupled split ring resonator (BC-SRR) loaded transmission lines to the design of rotary encoders for space applications', in 2016 IEEE MTT-S International Microwave Symposium (IMS), May 2016, pp. 1–4, doi: 10.1109/MWSYM.2016.7540017.

14. J. Joubert, 'Spiral microstrip resonators for narrow-stopband filters', Antennas Propag. IEE Proc. - Microw., vol. 150, no. 6, pp. 493–496, Dec. 2003, doi: 10.1049/ip-map:20031112.

15. J. D. Baena, R. Marqués, F. Medina, and J. Martel, 'Artificial magnetic metamaterial design by using spiral resonators', Phys. Rev. B, vol. 69, no. 1, p. 014402, Jan. 2004, doi: 10.1103/PhysRevB.69.014402.

16. S. Zahertar, A. D. Yalcinkaya, and H. Torun, 'Rectangular split-ring resonators with single-split and two-splits under different excitations at microwave frequencies', AIP Adv., vol. 5, no. 11, p. 117220, Nov. 2015, doi: 10.1063/1.4935910.

17. D. Brizi, N. Fontana, F. Costa, and A. Monorchio, 'Accurate Extraction of Equivalent Circuit Parameters of Spiral Resonators for the Design of Metamaterials', IEEE Trans. Microw. Theory Tech., vol. 67, no. 2, pp. 626–633, Feb. 2019, doi: 10.1109/TMTT.2018.2883036.

18. F. Bilotti, A. Toscano, and L. Vegni, 'Design of Spiral and Multiple Split-Ring Resonators for the Realization of Miniaturized Metamaterial Samples', IEEE Trans. Antennas Propag., vol. 55, no. 8, pp. 2258–2267, Aug. 2007, doi: 10.1109/TAP.2007.901950.

19. Y. Cheng and Y. Shu, 'A New Analytical Calculation of the Mutual Inductance of the Coaxial Spiral Rectangular Coils', IEEE Trans. Magn., vol. 50, no. 4, pp. 1–6, Apr. 2014, doi: 10.1109/TMAG.2013.2290972.

20. U. Jow and M. Ghovanloo, 'Modeling and Optimization of Printed Spiral Coils in Air, Saline, and Muscle Tissue Environments', IEEE Trans. Biomed. Circuits Syst., vol. 3, no. 5, pp. 339–347, Oct. 2009, doi: 10.1109/TBCAS.2009.2025366.

21. 'CST Studio Suite 3D EM simulation and analysis software'. https://www.3ds.com/products-services/simulia/products/cst-studio-suite/ (accessed Jan. 19, 2021).